

## Spinel $\text{LiMn}_2\text{O}_4$ /reduced graphene oxide hybrid for high rate lithium ion batteries

Seong-Min Bak,<sup>a</sup> Kyung-Wan Nam,<sup>\*b</sup> Chang-Wook Lee,<sup>a</sup> Kwang-Heon Kim,<sup>a</sup> Hyun-Chul Jung,<sup>c</sup> Xiao-Qing Yang<sup>b</sup> and Kwang-Bum Kim<sup>\*a</sup>

a. Department of Materials Science and Engineering, Yonsei University, 134 Shinchon-dong, Seodaemun-gu, Seoul 120-749, Republic of Korea.

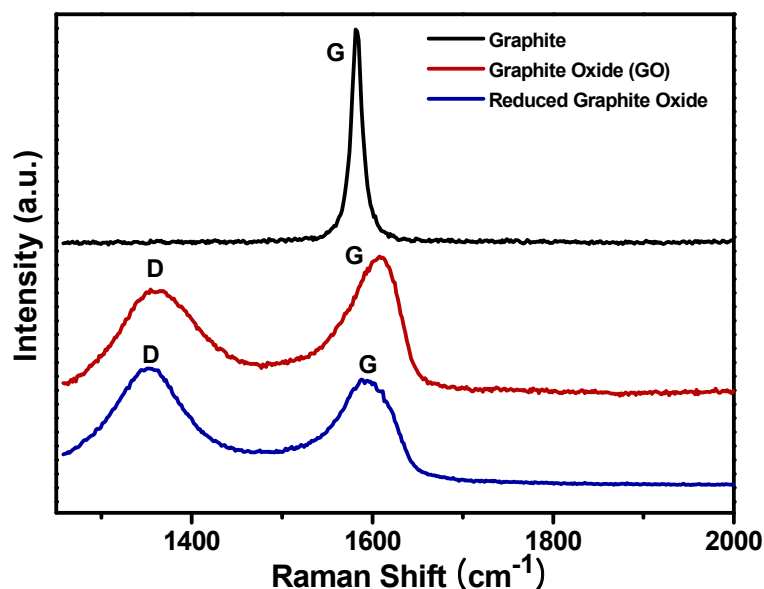
E-mail: kbkim@yonsei.ac.kr

b. Chemistry Department, Brookhaven National Laboratory, Upton, New York 11973, USA.

E-mail: knam@bnl.gov

c. Central R&D Institute, Samsung Electro-Mechanics Co.,LTD., Suwon, Gyunggi-do, 443-743, Republic of Korea.

**S1. Raman spectra of the Raman spectra of graphite (top), graphite oxide (middle), and the reduced graphene oxide (bottom).**

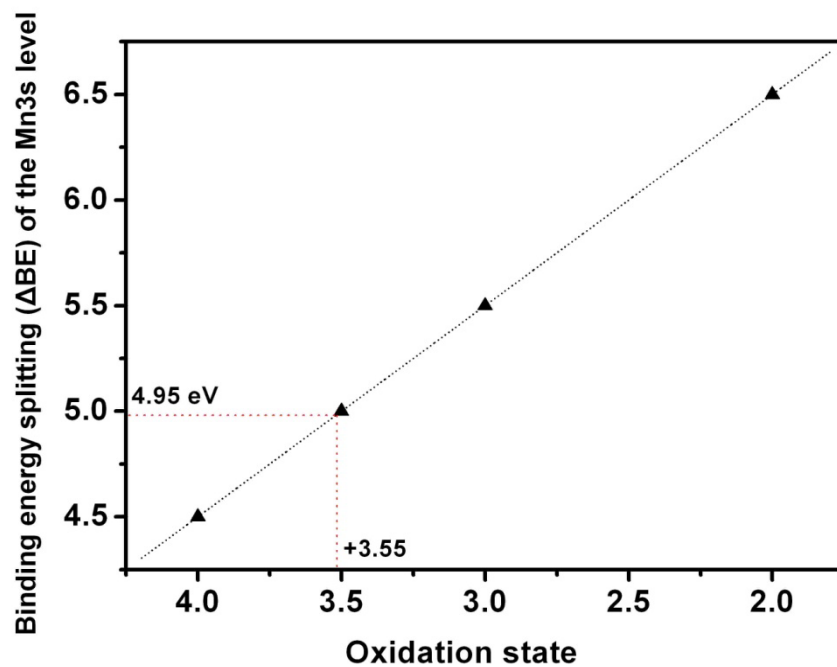


Raman spectroscopy provides information on the structural properties of carbonaceous materials, including disorder and defect structures. **S1** shows the Raman spectrum of pristine graphite, graphite oxide (GO) prepared using Hummers method and reduced graphene oxide (RGO)

prepared by chemical reduction using hydrazine as reducing agent. The significant structural changes occurring during the chemical processing of pristine graphite to GO, and then to the reduced GO, are reflected in their Raman spectrum. The Raman spectrum of the pristine graphite, as expected, displays a prominent G peak as the only feature at  $1581\text{ cm}^{-1}$ , corresponding to the first-order scattering of the E<sub>2g</sub> mode.[1] In the Raman spectrum of GO, the G band is broadened and shifted to  $1607\text{ cm}^{-1}$ . In addition, the D band at  $1363\text{ cm}^{-1}$  becomes prominent, indicating the reduction in size of the in-plane sp<sup>2</sup> domains, possibly due to the extensive oxidation. The Raman spectrum of the RGO also contains both G and D bands (at  $1589$  and  $1352\text{ cm}^{-1}$ , respectively), however, with an increased D/G intensity ratio compared to that in GO. S. Stankovich et al. reported that this change suggests a decrease in the average size of the sp<sup>2</sup> domains upon reduction of the exfoliated GO [1], and can be explained if new graphitic domains were created that are smaller in size to the ones present in GO before reduction, but more numerous in number.[2] Generally, RGO sheets which were produced through chemical exfoliation of natural graphite and hydrazine conversion would necessarily have some of defects in their structure.[3] The RGO material used in this study also has some of defects and disordered carbon structure. And the electrical conductivity ( $\sim 2 \times 10^2\text{ Sm}^{-1}$ ) and specific surface area (BET surface area:  $420\text{ m}^2\text{g}^{-1}$ ) are similar to RGO obtained in previous works using a hydrazine reduction.[2, 4] And elemental analysis (EA) revealed a C/O atomic ratio of 1.5 for GO and 10.6 for RGO after the chemical reduction.

In this study, RGO sheets with electrical conductivity of  $\sim 2 \times 10^2\text{ Sm}^{-1}$  and BET surface area of  $420\text{ m}^2\text{g}^{-1}$  served as an electronic conductive template for the LiMn<sub>2</sub>O<sub>4</sub> nanoparticles. We believe that RGO sheets used in this study is electrically conductive enough to ensure the excellent high rate capability of nano-sized LiMn<sub>2</sub>O<sub>4</sub>/RGO hybrid material as reported in the manuscript.

**S2. Oxidation number versus binding energy multiple splitting ( $\Delta BE$ ) of the Mn3s lines.**



**S3. Electrochemical properties of nano-sized LiMn<sub>2</sub>O<sub>4</sub>-based electrode materials prepared by various synthesis routes in the literature.**

Material	Synthetic method	Contents of conducting additive in working electrode	Specific capacity	Rate capability	Ref
Nanocrystalline spinel LiMn <sub>2</sub> O <sub>4</sub> (50-120 nm size)	Resorcinol-formaldehyde route	10 wt.% of acetylene black	136.9 mAh g <sup>-1</sup> at 0.2 C-rate	Decrease of 26 % (from 0.2 to 60 C-rate)	5
Nano-sized Li <sub>1.09</sub> Mn <sub>1.91</sub> O <sub>4</sub>	Spray pyrolysis	10 wt.% of acetylene black	107 mAh g <sup>-1</sup> at 1 C-rate	Decrease of 15% (from 1 to 10 C-rate)	6
Porous LiMn <sub>2</sub> O <sub>4</sub>	Biomimetic solution route	10 wt.% of acetylene black	135 mAh g <sup>-1</sup> at 0.7 C-rate	Decrease of 13% (from 0.7 to 3.5 C-rate)	7
LiMn <sub>2</sub> O <sub>4</sub> /C composite	Hydrothermal	10 wt.% of carbon black	102 mAh g <sup>-1</sup> at 0.04Ag <sup>-1</sup>	Decrease of 19% (from 0.04 to 2 Ag <sup>-1</sup> )	8
LiMn <sub>2</sub> O <sub>4</sub> /C nanocomposite	Flame co-synthesis	20 wt.% of super P (carbon black)	Over 80 mAh g <sup>-1</sup> at 50 C-rate	Decrease of 20% (from 5 to 50 C-rate)	9
LiMn <sub>2</sub> O <sub>4</sub> nanoparticle (7-26 nm size)	Flame spray pyrolysis	20 wt.% of super P (carbon black)	107.2 mAh g <sup>-1</sup> at 0.5 C-rate	Decrease of 20% (from 5 to 50 C-rate)	10
Single crystalline spinel LiMn <sub>2</sub> O <sub>4</sub> nanowire	Self templating of Na <sub>0.44</sub> MnO <sub>2</sub>	45 wt.% of acetylene black	108 mAh g <sup>-1</sup> at 5 Ag <sup>-1</sup>	Decrease of 19% (from 5 to 20 Ag <sup>-1</sup> )	11
Spinel LiMn <sub>2</sub> O <sub>4</sub> nanorods	Solid state reaction	10 wt.% of carbon black	110 mAh g <sup>-1</sup> at 0.1 C-rate	Decrease of 10% (from 0.1 to 1 C-rate)	12
Nano-LiMn <sub>2</sub> O <sub>4</sub> spinel	Resorcinol-formaldehyde route	12 wt.% of super S carbon	131 mAh g <sup>-1</sup> at 0.5 C-rate	Decrease of 15% (from 0.2 to 60 C-rate)	13
Spinel LiMn <sub>2</sub> O <sub>4</sub> nanoparticle	Hydrothermal	20 wt.% of acetylene black	108.3 mAh g <sup>-1</sup> at 0.8 C-rate	Decrease of 26% (from 0.8 to 16 C-rate)	14

## References

1. F. Tuinstra, J. L. Koenig, *J. Chem. Phys.*, 1970, 53, 1126.
2. S. Stankovich, D.A. Dikin, R.D. Piner, K.A. Kohlhaas, A. Kleinhammes, Y. Jia, Y. Wu, S.T. Nguyen, R.S. Ruoff, *Carbon*, 2007, 45, 1558.
3. (a) X. Gao, J. Jang, S. Nagase, *J. Phys. Chem. C*, 2010, 14, 832, (b) J.T. Robinson, F. K. Perkins, E.S. Snow, Z. Wei, P.E. Sheehan, *Nano Lett.*, 2008, 8, 3137.
4. (a) S.M. Paek, E.J. Yoo, I. Honma, *Nano Lett.*, 2009, 9, 72, (b) H. Kim, D.H. Seo, S. W. Kim, J. Kim, K. Kang, *Carbon*, 2011, 49, 326, (c) E.J. Yoo, J.D. Kim, E. Hosono, H.S. Zhou, T. Kudo, I. Honma, *Nano Lett.*, 2008, 8, 2277.
5. Y. Chen, K. Xie, Y. Pan, C. Zheng, *Solid State Ionics*, 2010, 181, 1445.
6. S. Hirose, T. Kodera, T. Ogihara, *J. Alloys and Compounds*, 2010, 506, 883.
7. H. Uchiyama, E. Hosono, H. Zhou, H. Imai, *J. Mater. Chem.*, 2009, 19, 4012.
8. H. Yue, X. Huang, D. Lv, Y. Yang, *Electrochim. Acta*, 2009, 54, 5363.
9. T.J. Patey, R. Buchel, S.H. Ng, F. Krumeich, S.E. Pratsinis, P. Novak, *J. Power Sources*, 2009, 189, 149.
10. T.J. Patey, R. Buchel, M. Nakayama, P. Novak, *Phys. Chem. Chem. Phys.*, 2009, 11, 3756.
11. E. Hosono, T. Kudo, I. Honma, H. Matsuda, H. Zhou, *Nano Lett.*, 2009, 9, 1045.
12. D.K. Kim, P. Muralidharan, H.W. Lee, R. Ruffo, Y. Yang, C.K. Chan, H. Peng, R.A. Huggins, Y. Cui, *Nano Lett.*, 2008, 11, 3948.
13. K.M. Shaju, P.G. Bruce, *Chem. Mater.*, 2008, 20, 5557.
14. C.H. Jiang, S.X. Dou, H.K. Liu, M. Ichihara, H.S. Zhou, *J. Power Sources*, 2007, 172, 410.